

Numerical study of direct contact membrane distillation process: Effects of operating parameters on TPC and thermal efficiency

Mohammadmehdi Zamaniasl*

Department of Mechanical Engineering, College of Engineering, Shahid Chamran University of Ahvaz, Ahvaz, Iran

(Received March 9, 2019, Revised May 27, 2019, Accepted June 27, 2019)

Abstract. Membrane distillation (MD) is one of the water treatment processes which involves the momentum, heat and mass transfer through channels and membrane. In this study, CFD modeling has been used to simulate the heat and mass transfer in the direct contact membrane distillation (DCMD). Also, the effect of operating parameters on the water flux is investigated. The result shows a good agreement with the experimental result. Results indicated that, while feed temperature is increasing in the feed side, water flux improves in the permeate side. Since higher velocity leads to the higher mixing and turbulence in the feed channel, water flux rises due to this increase in the feed velocity. Moreover, results revealed that temperature polarization coefficient is rising as flow rate (velocity) increases and it is decreasing while the feed temperature increases. Lastly, the thermal efficiency of direct contact membrane distillation is defined, and results confirm that thermal efficiency improves while feed temperature increases. Also, flow rate increment results in enhancement of thermal efficiency.

Keywords: computational fluid dynamic (CFD); heat transfer; water flux; temperature polarization coefficient (TPC); thermal efficiency; membrane distillation

1. Introduction

Nowadays, limited freshwater supplies in the world, and increasing water demand owing to the rapid population growth and economic growth have made a great challenge for a human being. Since 98% of water resources in the world are brackish water, so using cost-effective and efficient water treatment processes to overcome this issue seems an excellent solution. Among different water treatment operations, membrane distillation (MD) is a promising water treatment process which can provide us fresh water from saline water resources (Bahrami *et al.* 2018).

MD is a non-isothermal and membrane-based separation technology that heat and mass transfer influence each other. MD is operated due to the vapor pressure difference across the membrane. In this process, the hot brine flow as feed passes in one side of the porous membrane. Then, due to the hydrophobic nature of membrane only pure water vapor transports from pores of the membrane and condenses in the permeate side of the membrane. There are four different types of MD process, 1) direct contact MD (DCMD) 2) vacuum MD (VMD) 3) sweeping gas MD (SGMD) 4) air gap MD (AGMD). Among these MD types, DCMD as the simplest MD configuration has attracted considerable attentions. In DCMD hot and cold streams are in direct contact with the membrane and pure water will be collected through the cold flow.

Researchers have examined the MD process

experimentally since 1967, and in addition to the experimental investigations about the MD process, researchers have been using theoretical models to find the best models for MD modeling. Alsadi *et al.* investigated the vapor flux in the air gap membrane distillation both experimentally and theoretically. They suggested a theoretical model to predict the water flux and validated it with experimental results (Alsaadi *et al.* 2013). A numerical model of air gap MD conducted by Janajreh *et al.* to find the optimal performance of the air gap MD process. They have studied the effect of operating parameters on the thermal efficiency of air gap MD (Janajreh *et al.* 2017). Theoretical modeling and optimization of the sweeping gas membrane distillation have been studied by Khayet *et al.* (M Khayet, Cojocar, and Baroudi 2012). The vacuum membrane distillation is gained attention most recently, and it has been studied experimentally and numerically. Upadhyaya *et al.* (Upadhyaya *et al.* 2015) analyzed the vacuum MD using the mathematical and CFD modeling. Rana *et al.* investigated the mass and heat transfer in a vacuum membrane distillation and effect of feed temperature on the TPC in three types of modules (Rana *et al.* 2016). Li *et al.* (Li *et al.* 2018) carried out a numerical and experimental work to study the vacuum MD.

Although different types of theoretical models for DCMD has been carried out, CFD modeling of this process still is a significant challenge. In DCMD three different transport mechanisms are involved; Momentum, Heat, and mass transfer. Furthermore, as mentioned in DCMD heat transfer and mass transfer affect each other directly. This is the main reason that makes CFD modeling an issue. Dusty gas model in MD for prediction of water flux can be employed. This model has three mechanisms: Knudsen diffusion, viscous flow, and molecular diffusion. Another

*Corresponding author, B.Sc.
E-mail: mzamaniasl@gmail.com

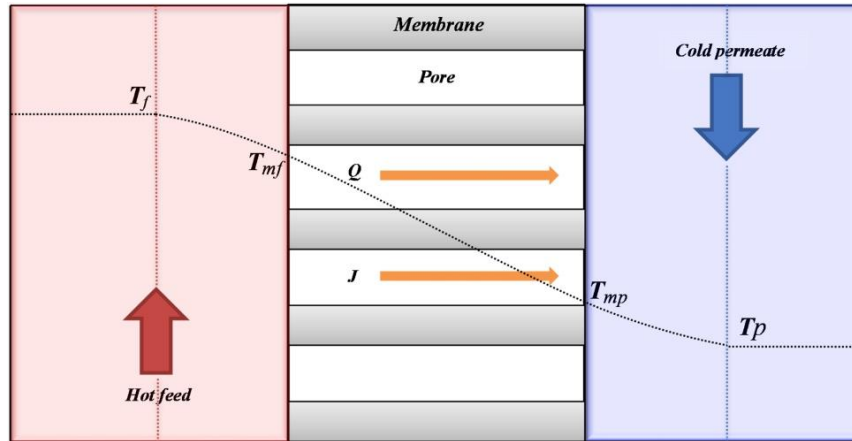


Fig. 1 Schematic of Heat and Mass transfer in DCMD process

method which can be considered to simulate the water desalination process in membranes is the resistance-in-series model (Qtaishat *et al.* 2008). Moreover, the Monte Carlo simulation model in MD also was used to simulate water transport through a hydrophobic porous membrane in DCMD. Chang *et al.* simulated a DCMD module using CFD to analyze the heat transfer coefficient in this module. He reported a good agreement of the experimental results of mass flux and simulated results (Chang, Ho, and Hsu 2016). D.U. Lawal and A.E. Khalifa developed an iterative procedure to predict the mass flux in the DCMD module with a primary focus on the membrane permeability effect on simulated mass flux result (U. Lawal and E. Khalifa 2014). Yu *et al.* used CFD to model heat transfer in a hollow fiber module in DCMD (Yu *et al.* 2011).

Moreover, the hollow fiber membrane module has been simulated by some researchers. Yang *et al.* analyzed the effect of different turbulence parameters in hollow fibers MD (Yang *et al.* 2012). Hwang *et al.* suggested a 2D model involving mass, heat, and momentum balance for predicting water flux in a flat-sheet module in the DCMD process (Hwang *et al.* 2011).

In MD, the temperature on the interface of the membrane in feed and permeate sections differ from the bulk temperature of hot and cold streams. This phenomenon is called temperature polarization and has a vital role in the performance of the membrane because it affects mass and heat transfer. The magnitude of temperature polarization is calculated by the temperature polarization coefficient (TPC). The TPC shows the dissipation of thermal energy owing to the thermal boundary layer resistance. Therefore, in this study, the effect of feed temperature and velocity variations on temperature polarization coefficient (TPC) the flat-sheet module direct contact membrane distillation has been investigated. Furthermore, CFD modeling has been used to investigate and validate the permeate flux in different feed flow rates, feed temperatures, and permeate temperatures. Finally, the thermal efficiency of direct contact membrane distillation process has been studied.

2. Theory

In DCMD, heat and mass transfer happens simultaneously. As it has been shown in Fig. 1, at feed side,

hot saline water enters the channel within specific velocity and temperature. Evaporated water molecule passes through the membrane, and it will be condensed at the permeate side.

2.1 Heat transfer

Heat transfer in direct contact membrane distillation process occurs in three steps. In the first step, heat will be transferred by convection from hot flow to the membrane surface. T_f stands for inlet temperature at the feed side. Using Newton's convection law at the feed side, Transferred heat can be written as

$$Q_f = h_f(T_f - T_{mf}) \quad (1)$$

where Q is Total Heat transfer, h_f is the convective heat transfer coefficient at the feed side, and T_{mf} is membranes surface temperature at the feed side. Convective heat transfer coefficient can be determined by the Nusslet number.

$$Nu = \frac{h \times d}{k} \quad (2)$$

where d is hydraulic diameter and k is thermal conductivity of feed fluid. Nusselt Number also can be estimated by empirical correlations. Based on flow regime, suitable Nusslet correlation can be chosen. In DCMD flow regime is considered as a laminar flow. Therefore, for laminar flow, following nusselt correlation has been used

$$Nu = 1.86 \times (Re \times Pr \times \left(\frac{d}{L}\right))^{0.33} \quad (3)$$

where Re and Pr are Reynolds numbers and Prandtl numbers respectively, and they defined as

$$Re = \frac{(\rho \times U \times dx)}{\mu} \quad (4)$$

$$Pr = \frac{(\mu \times C_p)}{k} \quad (5)$$

where ρ , μ , the U , and C_p are fluid density, the viscosity of the fluid, fluid velocity at feed side and specific heat capacity respectively.

In the case of the turbulent flow regime in channels, the below correlations are used to evaluate the Nusslet number (Khalifa *et al.* 2017)

$$Nu_f = 0.027 \times (Re^{0.8}) \times (Pr^{0.4}) \times \left(\frac{\mu_{bf}}{\mu_{mf}}\right)^{0.14} \quad (6)$$

$$Nu_p = 0.027 \times (Re^{0.8}) \times (Pr^{0.4}) \times \left(\frac{\mu_{mp}}{\mu_{bp}}\right)^{0.14} \quad (7)$$

The second step of heat transfer in DCMD is occurring in the membrane where heat transfers across the membrane by conduction. Furthermore, due to vapor transport from the membrane to the permeate side, total heat transfer in the membrane (Q_m) is the summation of conduction heat transfer across the membrane (Q_C) and transferred heat by latent heat of vaporization (Q_V), and it can be written as

$$Q_m = Q_C + Q_V \quad (8)$$

The conductive heat transfer in the membrane (Q_C) which is given by

$$Q_C = \left(\frac{K_m}{\delta}\right) \times (T_{mf} - T_{mp}) \quad (9)$$

where K_m and δ are thermal conductivity of membrane material and membrane thickness, respectively.

Different models have been used to estimate K_m , but the isostrain model is more often used. In this model, K_m is given by (Yu *et al.* 2011)

$$K_m = (k_g \times \varepsilon) + (1 - \varepsilon) \times k_p \quad (10)$$

where k_g is air thermal conductivity which is filling membrane pores, k_p is membrane material conductivity, and ε is membrane porosity.

Transferred heat by vapor molecules can be described as follow

$$Q_v = J \times \nabla H_v \quad (11)$$

where J and ∇H_v are vapor flux and latent heat of vaporization respectively;

Where latent heat of vaporization can be expressed by empirical correlations as below

$$\nabla H_v = 1.7535T + 2024.3 \quad (12)$$

where T is the feed temperatures in Kelvin.

Finally, the last step of heat transfer in the DCMD process is convective heat transfer from the membrane surface to permeate flow, and by Newton's law we can write it as follow

$$Q_p = h_p(T_{mp} - T_p) \quad (13)$$

where h_p and T_{mp} are convective heat transfer coefficient at permeate flow and membrane surface temperature at permeate side respectively. h_p can also be estimated with the same procedure that has been used for calculating h_f . The only difference is that Re and Pr have different values at the feed and permeate sides.

2.2 Mass transfer

Mass transfer in DCMD occurs by convection and vapor diffusion through the porous membrane. The vapor pressure difference is the driving force for mass transfer in MD.

Mass flux in MD can be expressed as

$$J_w = C_w \times \Delta P_m \quad (14)$$

where C_w and ΔP_m are the overall mass transfer coefficient and transmembrane vapor pressure difference respectively.

Transmembrane vapor pressure can be determined using the Antoine equation (Srisurichan, Jiratananon, and Fane 2006)

$$P_m = \exp\left(23.1964 - \frac{3816.44}{T_m - 46.13}\right) \quad (15)$$

Where T_m is membrane surface temperature in the feed and permeate side as below:

T_m at the feed side : T_{mf}

T_m at the permeate side: T_{mp}

Salinity effect should be considered in the vapor pressure in the feed solution. Therefore vapor pressure in the feed side can be written as

$$P_{mf} = \gamma_{wf} \times x_{wf} \times P_m \quad (16)$$

where γ_{wf} and x_{wf} are activity coefficient and mole fraction of water in feed, respectively.

For a NaCl aqueous solution, the activity coefficient is determined as

$$\gamma_{wf} = 1 - (0.5 \times x_{NaCl}) - (10 \times x_{NaCl}^2) \quad (17)$$

where x_{NaCl} is mole fraction of NaCl in the water solution.

Mass transfer coefficient (Membrane permeability, C_w) depends on the vapor diffusion region in the mass transfer process. Based on Knudsen numbers value; three diffusion region can be considered for vapor transport through the membrane. Knudsen number is described as

$$Kn = \frac{\lambda_w}{d_p} \quad (18)$$

where λ_w is mean free path of water molecules and d_p is pores size (diameter). λ_w is expressed as

$$\lambda_w = \frac{K_B \times T}{\sqrt{2} \times \pi \times P_m \times (2.641 \times 10^{-10})^2} \quad (19)$$

where K_B is Boltzmann constant, T is the absolute mean Temperature in pores(kelvin) and P_m is mean pressure in membrane pores.

When the mean free path is less than the membrane pore size ($Kn < 0.01$ or $d_p > 100 \times \lambda_w$) the molecular diffusion is the responsible mechanism for vapor transport through the membrane. In this case, the mass transfer coefficient is stated as (Qtaishat *et al.* 2008)

$$C_w^D = \frac{\pi PD_w r_D^2}{RT P_a \tau \delta} \quad (20)$$

If membrane pores assumed to have a uniform size, the above equation could be written as

$$C_w^D = \frac{\varepsilon PD_w M_w}{\tau \delta P_a RT} \quad (21)$$

where R is gas constant, τ is membrane tortosity, P_a is the air pressure in the membrane, P is total pressure inside

Table 1 Module properties

Symbol	ε	δ	d_p	L	H	W	A	d_h	R	k_g	k_p
Value	80 (%)	154 (μm)	45 (μm)	66 (mm)	5 (mm)	24 (mm)	120 (mm^2)	0.00827 (mm)	8.314 (J/Kmol)	0.029 (W/mK)	0.259 (W/mK)

the pore of membrane and D_w is the diffusion coefficient which can be calculated from the equation below

$$PD_w = 1.895 \times 10^{-5} T^{2.072} \quad (22)$$

where PD_w is in $\text{Pa}\cdot\text{m}^2/\text{s}$.

Macki-Meares suggested the below equation for estimating the membrane tortuosity (Srisurichan, Jiratananon and Fane 2006)

$$\tau = \frac{(2 - \varepsilon)^2}{\varepsilon} \quad (23)$$

When the mean free path of vapor is more than the membrane pore size ($\text{Kn} > 10$ or $d_p < 0.1 \times \lambda_w$), vapor molecules will be transported by Knudsen diffusion across the membrane. In this case, membrane permeability is given by

$$C_w^K = \frac{2\pi}{3} \frac{1}{RT} \left(\frac{8RT}{\pi M_w} \right)^{\frac{1}{2}} \frac{r_k^3}{\tau \delta} \quad (24)$$

With the assumption of uniform size for membrane pore, the above equation can be written as

$$C_w^K = \frac{2}{3} \frac{\varepsilon \bar{r}_k}{RT \tau \delta} \left(\frac{8RT}{\pi M_w} \right)^{0.5} \quad (25)$$

If we have $0.01 < \text{Kn} < 10$ (or $0.1\lambda_w < d_p < 100\lambda_w$) transition region will happen which in this region both of Knudsen and molecular diffusion are responsible for vapor transport through membrane pore. Combining the two diffusion type and using uniform size assumption for membrane pores, membrane permeability in the transition region is given as (Mohamed Khayet 2011)

$$C_w^c = \frac{1}{RT\delta} \left[\frac{3}{2} \frac{\tau}{\varepsilon r} \left(\frac{\pi M_w}{8RT} \right)^{\frac{1}{2}} + \frac{P_a \tau}{\varepsilon PD_w} \right]^{-1} \quad (26)$$

3. Modeling

For DCMD modeling the below assumptions are made;

- The steady state flow condition
- No heat loss from the module to the atmosphere
- Membrane geometrical properties such as thickness, membrane pore size, porosity, and tortuosity are constant.
- Concentration effect on the specific heat of evaporation and condensation has been neglected.

Since we assumed there is no heat loss from the MD module to the atmosphere, transferred heat can be given as

$$Q_f = Q_m = Q_p \quad (27)$$

where

$$Q_m = Q_c + Q_v$$

Combining Eqs. (1), (8), (9) and (13) leads to

$$h_f(T_f - T_{mf}) = \frac{K_m}{\delta} (T_{mf} - T_{mp}) + J\Delta H_w = h_p(T_{mp} - T_p) \quad (28)$$

Finally, by manipulation of the above equation

$$T_{mf} = \frac{\frac{K_m}{\delta} (T_p + \frac{h_f}{h_p} T_f) + h_f T_f - J\Delta H_w}{\frac{K_m}{\delta} + h_f (1 + \frac{K_m}{\delta h_p})} \quad (29)$$

$$T_{mp} = \frac{\frac{K_m}{\delta} (T_f + \frac{h_p}{h_f} T_p) + h_p T_p - J\Delta H_w}{\frac{K_m}{\delta} + h_p (1 + \frac{K_m}{\delta h_f})} \quad (30)$$

where h_f and h_p are evaluated by Eqs. (2)-(7).

An iterative procedure is implemented in Matlab to calculate vapor mass flux, T_{mf} and T_{mp} .

4. Results and discussion

4.1 Effects of operating parameters and model validation

For model validation, the result of A. Khalifa's *et al.* experimental work is used to prove that modeling has been carried out correctly (Khalifa *et al.* 2017). Table 1 Shows the module properties of the PTEE (45 μm) membrane in A. Khalifa's research work. These properties are used for the modeling process.

Fig. 2 shows the comparison of permeate flux against the feed temperature in experimental work and conducted model. The result of modeling is in a good agreement with the experimental result. As expected, the permeate flux increases with the increase of the feed temperature. This behavior is because of the effect of temperature on the vapor pressure. By increasing the feed temperature, vapor pressure rises exponentially, and due to this increase in the vapor pressure, water flux is growing too.

In order to investigate the effect of permeate temperature on water flux, water flux is evaluated at different permeate temperatures (see Fig. 3). As Fig. 3 shows, water flux improves with permeate temperature decrement. Since decreasing the permeate temperature increases the transmembrane vapor pressure difference, water flux enhances.

Flow rate effect vs. water flux has been validated against A. Khalifa's experimental result to support the modeling accuracy in this work. Modeling and experimental

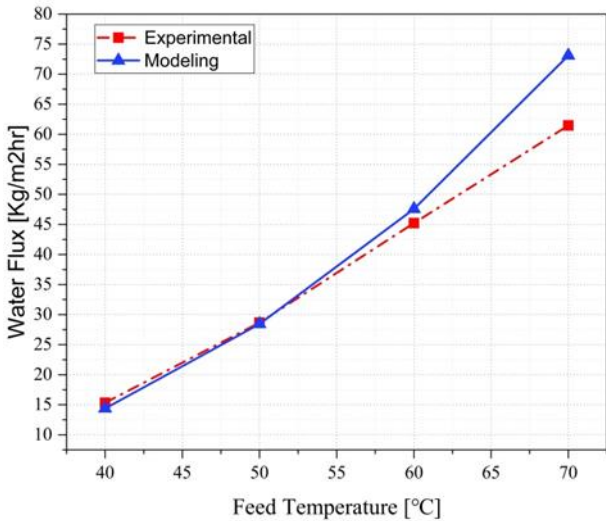


Fig. 2 Modeling and experimental result of the Feed Temperature effect on water flux. Feed, permeate flow rate, feed concentration and permeate temperature is 4.6 [L/min], 3.65[L/min], 2 g/L and 20°C respectively.

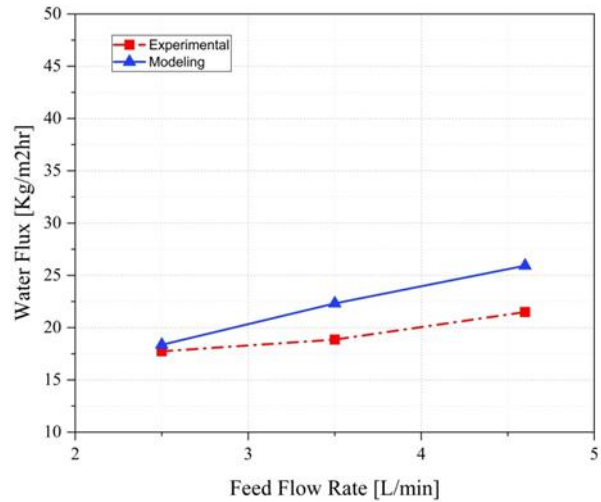


Fig. 4 Effect of feed flow rate vs. water flux. Feed concentration, feed and permeate temperatures are 2 g/L, 50 °C and 25 °C respectively. Permeate flow rate is 3.65 [L/min]

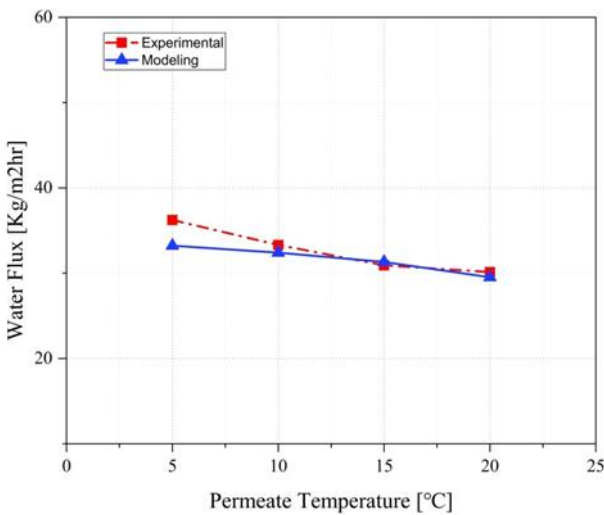


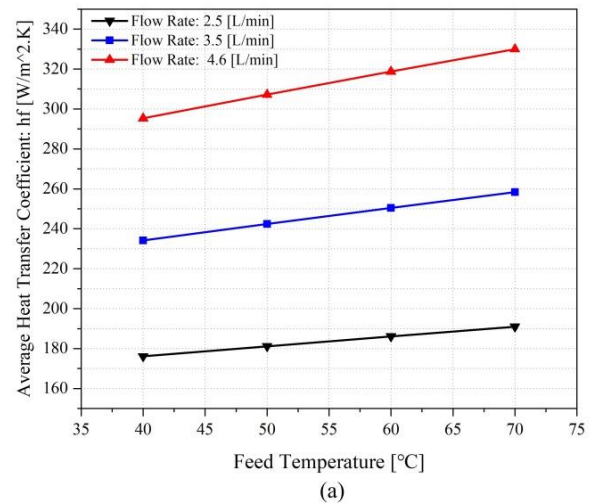
Fig. 3 Water flux at different permeate temperature: feed flow rate 4.6[L/min], permeate flow rate 3.65[L/min], feed concentration 2 g/L, feed temperature 50 [°C]

results are in good agreement. Fig. 4 demonstrates that with a higher flow rate in the feed channel, higher turbulent is expected, and it leads to higher mixing in the feed side and decreases the thickness of temperature boundary layer and increases the water flux in the permeate channel.

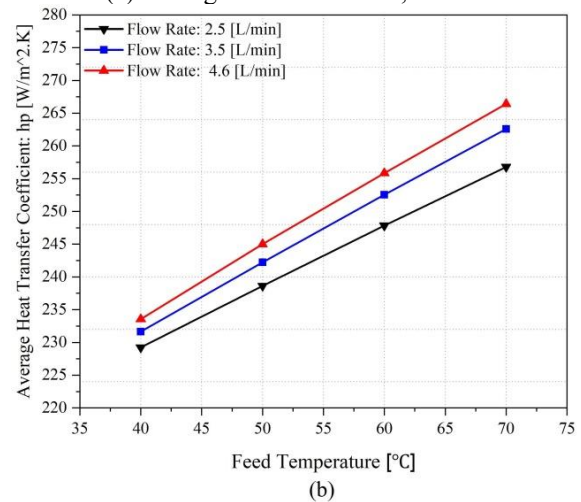
Fig. 5(a)-(b) illustrate the average heat transfer coefficients in the feed (h_f) and permeate (h_p) sides. The average heat transfer coefficients of boundary layers in both feed and permeate streams are increased as the flow rate increases. The global film heat transfer coefficient (h_{film}) can be determined as below (Yazgan-birgi, Hassan, and Arafat 2018)

$$\frac{1}{h_{film}} = \frac{1}{h_f} + \frac{1}{h_p}$$

As Fig. 6 indicates the global film heat transfer



(a) Average heat coefficient; feed side



(b) Average heat coefficient; permeate side

Fig. 5 Average heat transfer coefficient vs. feed flow rate (a) in the feed side: h_f (b) in the permeate side: h_p . Permeate flow rate 3.65 [L/min], permeate temperature 20°C

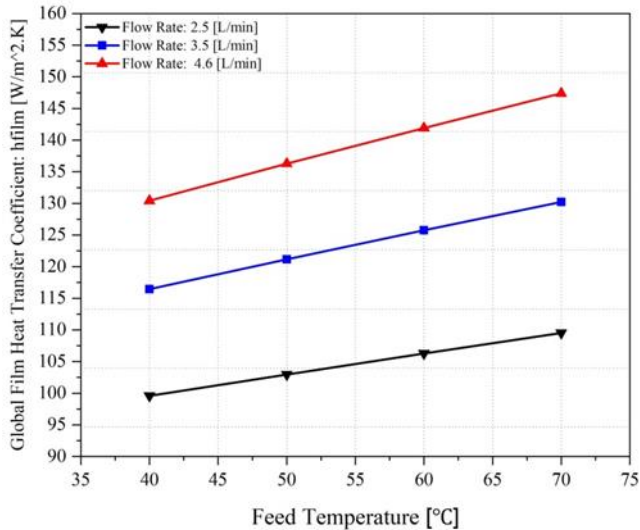


Fig. 6 Global film heat transfer coefficient versus flow rate. Permeate flow rate 3.65 [L/min], permeate temperature 20°C

coefficient is also increasing with the increment of the flow rate. These upturns in the heat transfer coefficients enhance the TPC value, consequently.

4.2 Temperature polarization coefficient

The temperature difference between the two sides of the membrane surface is created by temperature polarization phenomena. Temperature polarization causes the temperature difference between the surface temperature of the membrane and bulk temperature of feed and permeates flows. Temperature polarization coefficient is defined as below

$$TPC = \frac{T_{mf} - T_{mp}}{T_f - T_p} \quad (31)$$

In a well-designed system, T_{mf} and T_{mp} should approach to T_f and T_p respectively. Therefore TPC converges to 1, and this means temperature polarization is decreasing and driving force and flux are increasing (Zahirifar *et al.* 2018).

Effect of feed temperature on the temperature polarization coefficient is showed in Fig. 7. It can be seen that temperature polarization decreases while feed temperature is increasing (see Fig. 7). This happens due to the exponential change of vapor pressure in the feed side by rising the feed temperature. This exponential growth of vapor pressure makes a higher mass flux in the membrane, and higher mass flux requires higher heat flux in the liquid phases which increases the gradient of temperature in the liquid boundary layers and the temperature polarization.

TPC vs. Flow rate has been investigated in Fig. 8. It shows that TPC is increasing as the flow rate increases in the feed side. Growing flow rate means higher velocity in the channel. As velocity rises the turbulent flow regime grows in the channel, and it causes the thermal boundary reduction, in this way T_{mf} is increasing to approach to

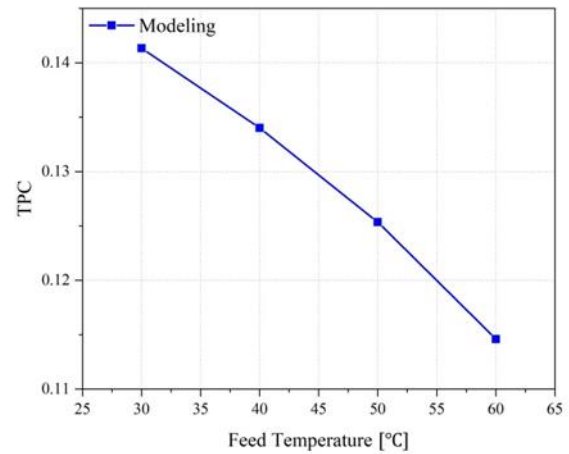


Fig. 7 TPC vs. Feed temperature. Flow rate in the feed and permeate side is 1.6 [L/min]. Permeate temperature is 20°C

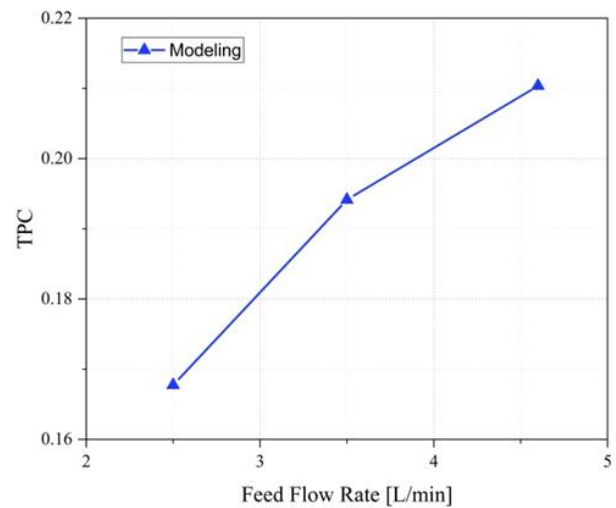


Fig. 8 TPC vs. Flow rate. Permeate flow rate, Feed temperature, and the permeate temperature are 3.65 [L/min], 40°C and 20°C respectively

T_f and T_{mp} is approaching to T_p (Abdel-Rahman 2008).

4.3 Thermal efficiency

Thermal efficiency (TE) in direct contact membrane distillation can be determined as below

$$TE(\%) = \frac{J * H_v}{J * H_v + \frac{K_m}{\delta} (T_{fm} - T_{pm})} \times 100 \quad (32)$$

Which is the ratio between the transported heat by vapors to the total transported heat through the membrane (Ali *et al.* 2013).

Thermal efficiency is reported in Fig. 9 at various feed temperatures. Thermal efficiency enhances as feed temperature increases, and it is due to an increase in the ΔT_m which leads to different in the vapor transport across the membrane. Additionally, thermal efficiency is shown in Fig. 10 at different flow rates. Since higher flow rate improves the water flux and turns the flow regime to

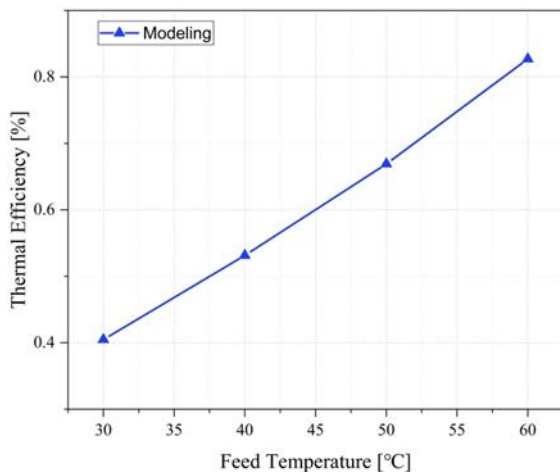


Fig. 9 Thermal efficiency against the various feed temperatures. Feed flow rate 4.6 [L/min], permeate flow rate 3.65 [L/min], permeate temperature 20°C

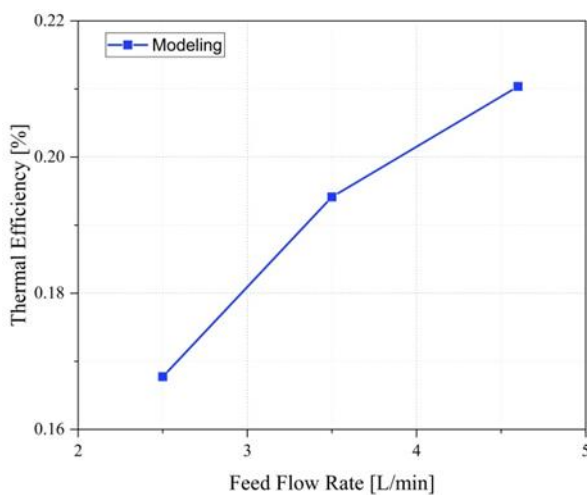


Fig. 10 Thermal efficiency vs. flow rate. Feed temperature 40°C, permeate temperature 20°C, permeate flow rate 3.65 [L/min]

turbulent, thermal efficiency enhances with increasing the flow rate. Nevertheless, this improvement reduces as the flow rate goes higher. This reduction relates to the decline of heat transfer efficiency between the flow and the membrane surface (Salem *et al.* 2019).

5. Conclusion

A numerical model was conducted in this work to simulate the direct contact membrane distillation process. Effect of flow rate, feed and permeate temperatures on the permeate flux are investigated and validated against the experimental works, and it showed a good agreement between the modeling and experimental results. Temperature polarization and thermal efficiency also were defined, and the effect of flow rate and feed temperature on the temperature polarization coefficient (TPC) and thermal efficiency was studied. The results indicate that:

- Water flux increases by increasing the feed temperature, and it is because of that as feed temperature increases, the vapor pressure grows exponentially and thereby, the flux increases too.
- As flow rate raises in the feed side, water flux increases due to this fact that higher flow rate means higher velocity and higher velocity causes the turbulent regime to appear in the feed flow and makes the temperature boundary layer thicker.
- Temperature polarization is an essential factor in vapor transfer through the membrane. Therefore by defining the temperature polarization coefficient (TPC), the effect of operation condition on temperature polarization evaluated.
- TPC is reducing as feed temperature increases, and it rises while the flow rate is increasing.
- Thermal efficiency improves with increasing the flow rate and also with feed temperature ascension although this enhancement is more affected by feed temperature than flow rate.
- Since increasing the feed temperature increases the thermal efficiency and water flux in direct contact membrane distillation process, it can be used as the major parameter for enhancing the system performance although it must be mentioned that rising the feed temperature decreases the TPC. Therefore, an optimal model should be considered in this subject.

References

- Abdel-Rahman, A. (2008), "Modeling Temperature and Salt Concentration Distribution in Direct Contact Membrane Distillation", *Faculty.Ksu.Edu.Sa* 36(5): 1167–88. http://faculty.ksu.edu.sa/72005/Papers_of_Interest_Water/Modeling_Temperature_and_Salt_Concentration_Distribution.pdf.
- Ali, A., Macedonio, F., Drioli, E., Aljlil, S., & Alharbi, O. A. (2013), "Experimental and Theoretical Evaluation of Temperature Polarization Phenomenon in Direct Contact Membrane Distillation", *Chem. Eng. Res. Design*, 91(10), 1966–1977. <http://dx.doi.org/10.1016/j.cherd.2013.06.030>.
- Alsaadi, A.S., Ghaffour, N., Li, J.D., Gray, S., Francis, L., Maab, H., and Amy, G.L. (2013), "Modeling of air-gap membrane distillation process: A theoretical and experimental study", *J. Membr. Sci.*, 445, 53–65. <https://doi.org/10.1016/j.memsci.2013.05.049>.
- Bahrami, M., Karimi-Sabet, J., Hatamnejad, A., Dastbaz, A., & Moosavian, M.A. (2018), "Optimization and modification of PVDF dual-layer hollow fiber membrane for direct contact membrane distillation; Application of response surface methodology and morphology study", *Korean J. Chem., Eng.*, 35(11), 2241–2255. <https://doi.org/10.1007/s11814-018-0038-4>.
- Chang, H., Ho, C.D. and Hsu, J.A. (2016), "Analysis of heat transfer coefficients in direct contact membrane distillation modules using CFD simulation", *J. Appl. Sci. Eng.*, 19(2), 197–206.
- Hwang, H.J., He, K., Gray, S., Zhang, J. and Moon, I.S. (2011), "Direct Contact Membrane Distillation (DCMD): Experimental Study on the Commercial PTFE Membrane and Modeling", *J. Membr. Sci.*, 371(1–2), 90–98. <https://doi.org/10.1016/j.memsci.2011.01.020>.
- Janajreh, I., El Kadi, K., Hashaikeh, R. and Ahmed, R. (2017), "Numerical investigation of air gap membrane distillation (AGMD): Seeking optimal performance", *Desalination*

424(October), 122-130. <http://doi.org/10.1016/j.desal.2017.10.001>.

Khalifa, A., Ahmad, H., Antar, M., Laoui, T. and Khayet, M. (2017), "Experimental and theoretical investigations on water desalination using direct contact membrane distillation", *Desalination* **404**, 22-34. <http://doi.org/10.1016/j.desal.2016.10.009>.

Khayet, M., Cojocar, C. and Baroudi, A. (2012), "Modeling and optimization of sweeping gas membrane distillation modeling and optimization of sweeping gas membrane distillation", *Desalination* **287**(February), 159-166. <http://doi.org/10.1016/j.desal.2011.04.070>.

Khayet, Mohamed (2011), "Membranes and theoretical modeling of membrane distillation: A review", *Adv. Colloid Interface Sci.* **164**(1-2), 56-88. <http://dx.doi.org/10.1016/j.cis.2010.09.005>.

Li, Z., Rana, D., Wang, Z., Matsuura, T. and Lan, C.Q. (2018), "Synergic effects of hydrophilic and hydrophobic nanoparticles on performance of nanocomposite distillation membranes: An experimental and numerical study", *Separation Purification Technol.*, **202**, 45-58. <https://doi.org/10.1016/j.seppur.2018.03.032>.

Qtaishat, M., Matsuura, T., Kruczek, B. and Khayet, M. (2008), "Heat and mass transfer analysis in direct contact membrane distillation", *Desalination*, **219**(1-3), 272-292. <https://doi.org/10.1016/j.desal.2007.05.019>.

Rana, D., Yang, Y., Matsuura, T. and Lan, C.Q. (2016), "The heat and mass transfer of vacuum membrane distillation: Effect of active layer morphology with and without support material", *Separation Purification Technol.*, **164**, 56-62. <http://dx.doi.org/10.1016/j.seppur.2016.03.023>.

Salem, M. S., El-shazly, A. H., Nady, N., Elmarghany, M. R., Shouman, M. A. and Sabry, M. N. (2019), "33-D numerical investigation on commercial PTFE membranes for membrane distillation: Effect of inlet conditions on heat and mass transfer", *Case Studies Thermal Eng.*, **13**, <https://linkinghub.elsevier.com/retrieve/pii/S2214157X18304210>.

Srisurichan, S., Ratana J. and Fane, A.G. (2006), "Mass transfer mechanisms and transport resistances in direct contact membrane distillation process", **277**, 186-194. <https://doi.org/10.1016/j.memsci.2005.10.028>.

Lawal, D. U. and Khalifa, A. E. (2014), "Flux prediction in direct contact membrane distillation", *J. Mater. Mech. Manufact.*, **2**(4), 302-308. www.ijmmm.org/index.php?m=content&c=index&a=show&catid=33&id=182.

Upadhyaya, S., Singh, K., Chaurasia, S.P. and Dohare, R.K. (2015), "Mathematical and CFD modeling of vacuum membrane distillation for desalination", *Desalination Water Treat.*, **57**(May 2016-26), 37-41. <https://doi.org/10.1080/19443994.2015.1048306>.

Yang, X., Yu, H., Wang, R. and Fane, A.G. (2012), "Optimization of microstructured hollow fiber design for membrane distillation applications using CFD modeling", *J. Membr. Sci.*, **421-422**, 258-270. <http://doi.org/10.1016/j.memsci.2012.07.022>.

Yazgan-birgi, P., Hassan, M.I. and Arafat, H.A. (2018), "Comparative performance assessment of flat sheet and hollow fiber DCMD processes using CFD modeling separation and purification technology comparative performance assessment of flat sheet and hollow fiber DCMD processes using CFD modeling", *Separation Purification Technol.*, **212**(November): 709-722. <https://doi.org/10.1016/j.seppur.2018.11.085>.

Yu, H., Yang, X., Wang, R. and Fane, A.G. (2011), "Numerical simulation of heat and mass transfer in direct membrane distillation in a hollow fiber module with laminar flow", *J. Membr. Sci.*, **384**(1-2), 107-116. <http://doi.org/10.1016/j.memsci.2011.09.011>.

Zahirifar, J., Karimi-Sabet, J., Moosavian, S. M. A., Hadi, A. and Khadiv-Parsi, P. (2018), "Fabrication of a novel octadecylamine functionalized graphene oxide/PVDF dual-layer flat sheet

membrane for desalination via air gap membrane distillation", *Desalination*, **428**(May 2017), 227-239. <https://doi.org/10.1016/j.desal.2017.11.028>.

Nomenclature

A	Cross-sectional area [m ²]
d_p	Pore size [μm]
d_h	Hydraulic diameter [m]
D	Diffusion coefficient [m ² /s]
h	Heat transfer coefficient [W/m ² K]
∇H_v	Heat of vaporization [kJ/kg]
J_w	Permeate flux [kg/m ² hr]
K	Thermal conductivity [W/mK]
C_w	Mass transfer coefficient [kg/m ² sPa]
K_m	Membrane thermal conductivity [W/mK]
K_g	Thermal conductivity of gas filling the pores [W/mK]
K_p	Thermal conductivity of membrane material [W/mK]
Kn	Knudsen number [dimensionless number]
M_w	Molecular weight [g/mol]
Nu	Nusselt Number [dimensionless number]
P	Total pressure [Pa]
P_m	Mean Pressure [Pa]
Pr	Prandtl Number [dimensionless number]
Q_v	Latent heat transfer [W/m ²]
Q_c	Conduction heat transfer [W/m ²]
R	Gas constant [J/Kmol]
Re	Reynolds number [dimensionless number]
T	Absolute temperature [K]
C_p	Specific heat [KJ/Kg.K]
x	Mole fraction
K_B	Boltzmann constant [1.3807×10^{-23} J/K]

Subscripts and Superscripts:

f	Feed
p	Permeate
m	Membrane
b	Bulk
mf	Feed side of the membrane
mp	Permeate side of the membrane
bf	Bulk feed
bp	Bulk permeate
c	Permeate side
h	Feed side

Greek Letters:

γ	Salt activity coefficient
δ	Membrane thickness [μm]
ε	Porosity [%]
τ	Tortuosity [No unit]
μ	Viscosity [Pa.s]
λ	Mean free path [m]
ρ	Density [kg/m ³]

CC